PLOS ONE

RESEARCH ARTICLE

Prediction of formation force during single-point incremental sheet metal forming using artificial intelligence techniques

Ali Alsamhan, Adham E. Ragab, Abdulmajeed Dabwan*, Mustafa M. Nasr, Lotfi Hidri

King Saud University, Industrial Engineering Department, King Saud University, Riyadh, Saudi Arabia

* abmj999@yahoo.com

Check for updates

OPEN ACCESS

Citation: Alsamhan A, Ragab AE, Dabwan A, Nasr MM, Hidri L (2019) Prediction of formation force during single-point incremental sheet metal forming using artificial intelligence techniques. PLoS ONE 14(8): e0221341. https://doi.org/10.1371/journal.pone.0221341

Editor: Jie Zhang, Newcastle University, UNITED KINGDOM

Received: April 24, 2019

Accepted: August 5, 2019

Published: August 22, 2019

Copyright: © 2019 Alsamhan et al. This is an open access article distributed under the terms of the Creative Commons Attribution License, which permits unrestricted use, distribution, and reproduction in any medium, provided the original author and source are credited.

Data Availability Statement: All relevant data are within the manuscript.

Funding: Deanship of Scientific Research at King Saud University funding this work through research group No (RG- 1439-56).

Competing interests: The authors have declared that no competing interests exist.

Abbreviations: ANFIS, Adaptive neuro-fuzzy inference system; ANN, Artificial neural network; Dsigmf, Difference of two fuzzy sigmoid

Abstract

Single-point incremental forming (SPIF) is a technology that allows incremental manufacturing of complex parts from a flat sheet using simple tools; further, this technology is flexible and economical. Measuring the forming force using this technology helps in preventing failures, determining the optimal processes, and implementing on-line control. In this paper, an experimental study using SPIF is described. This study focuses on the influence of four different process parameters, namely, step size, tool diameter, sheet thickness, and feed rate, on the maximum forming force. For an efficient force predictive model based on an adaptive neuro-fuzzy inference system (ANFIS), an artificial neural network (ANN) and a regressions model were applied. The predicted forces exhibited relatively good agreement with the experimental results. The results indicate that the performance of the ANFIS model realizes the full potential of the ANN model.

Introduction

Incremental sheet forming (ISF) is a flexible manufacturing technology that does not require special dies and uses a single tool to produce a variety of regular and multifaceted shapes. Further, it is economical when employed in the manufacturing of complex parts using simple tools as compared with other conventional sheet metal forming technologies (e.g., extrusion, hydroforming [1], and deep drawing [2]) because it does not require expensive dies or punches. In addition, it is used as a simple tool to incrementally develop the desired parts from sheets. However, it is time-consuming and thus not useful for mass production.

The ISF technique can be separated into two classes: two-point incremental forming (TPIF), which requires a partial die as a support for the sheet during the process [3], and single-point incremental forming (SPIF), which does not require any specific die [4]. Currently, focus is on SPIF, in which a small hemispherical tool is used to mold the sheet into the desired shapes; the tool is driven using a computer numerical control (CNC) machine along a predefined toolpath generated through computer-aided manufacturing software. The peripheral of the sheet is clamped using a fixture. Through this technique, complex parts can be manufactured in small batches and prototypes can be economically obtained.

membership functions; Fx, forming force on x-axis; Fy, forming force on y-axis; Fz, forming force on z-axis; Gaussmf, Gaussian membership function; Gbellmf, Generalized bell membership function; MAPE, Mean absolute percentage error; Psigmf, Product of two sigmoidal functions; Trapmf, Grapezoidal membership function; Trimf, Triangular membership functions.

ISF is used in many applications, such as the manufacturing of automotive parts [5] and the standardization of void nucleation models for automotive aluminum sheets [6]. Furthermore, it can be used to produce parts such as a palate or knee implants [7] or an ankle prosthesis [8] [9]. The forming force in SPIF is essential while utilizing machines adapted for processes such as robots and milling centers [3]. It helps determine the optimal process parameters and equipment suitable for sheet forming [10]. The forming force has characteristics that are essential in predicting the power of a machine; in addition, it helps with the design of tools and improves the understanding of the deformation mechanics of several processes [11]. Iseki [12] was among the first few researchers to determine the forming forces for a pyramid based on a plane–strain deformation using a simple approximated deformation analysis. Later, Jeswiet et al. [13] measured the force magnitudes of SPIF and TPIF pyramids and truncated cones. Filice et al. [14] worked on a force analysis and categorized the force trends of a tangential force into three categories, namely, monotonically reducing, polynomial, and steady-state force trends. Dabwan [15] showed that the sheet thickness is the main factor in estimating the forming force, followed by the tool diameter and step size. The feed rate has proven to be insignificant in estimating the forming force. Duflou et al. [16] found that the forming forces increase with the sheet thickness, wall angle, and step size. Kumar and Gulati [17] investigated and optimized the effects of input factors on the forming forces using the Taguchi approach and analysis of variance. They showed that the force trend after the peak values depends on the instant input factors, which can be categorized into sets of parameters such as safe, severe, and crucial. Bagudanch et al. [18] concluded that the forming force is influenced by the bending condition. They also found that the forming force decreases as the spindle speed increases. Arfa et al. [19] and Henrard et al. [20] used a finite element analysis to predict the SPIF forces with satisfactory precision. Ingarao et al. [21] calculated and estimated the energy consumption for the SPIF process based on the recorded force data. Petek et al. [22] studied and localized the fracture by analyzing the response force using a skewness function. Fiorentino [23] presented another failure criterion according to the force detected during the forming process. Moreover, Ambrogio et al. [24] proposed that the incremental increase in force required to reach its maximum value can be effectually used as a predecessor to failure in SPIF.

Therefore, it is essential to model and quantify the relationship between the forming force and the input process parameter affecting its value. Further, empirical models developed using traditional methods may not describe the nonlinear complex relationship between the input and output variables. Fuzzy logic (FL), an artificial neural network (ANN), and a genetic algorithm are unconventional methods used to develop models for a nonlinear complex system. An adaptive neuro-fuzzy inference system (ANFIS) can be used in numerous fields such as manufacturing technologies, machining, and economic systems [25]. ANFIS is a type of ANN developed based on a Takagi–Sugeno FIS. This approach was developed during the 1990s. ANFIS is a combination of neural networks and FL principles, and can capture the benefits of both in a single framework [26]. The inference system corresponding to the set of fuzzy IF-THEN rules can approximate nonlinear functions [27]. Therefore, ANFIS is considered a comprehensive estimator.

An investigation into the forming forces in SPIF is particularly important for selecting the appropriate hardware and optimizing the process parameters to assure the precision of a process. The efficient prediction of the forming forces is desirable in order to monitor the forming process, prevent failures, and implement on-line process control. The characterization of the forming forces is essential in order to estimate the needed power of the machine. The expected forming force has consequences regarding the design of the tooling and fixtures, as well as on the selected machine. There has recently been an increasing interest in the development of models that can help investigate the effects of input variables on the performance outputs

Table 1. Chemical composition of AA1050-H14 sheets used in this study.

Sample	Al %	Fe %	Si %	Ti %	Other
1	99.5	0.368	0.0480	0.0216	0.0624
2	99.5	0.360	0.0496	0.0205	0.0007

https://doi.org/10.1371/journal.pone.0221341.t001

using artificial intelligence methods as an alternative to traditional approaches [28]–[31]. This paper proposes an intelligent process model, founded on the concept of data mining, for predicting the forming forces in SPIF. Several researchers have addressed the limitations of this process, resulting in low-quality profile products. The predictive model for the forming forces described in this paper is based on an adaptive-neuro fuzzy inference system (ANFIS) and an artificial neural network (ANN), which have not been considered in previous studies to the best of our knowledge. An accurate model used to predict the forming forces in SPIF is essential in order to control the process quality.

The rest of this paper is organized as follows: The experiments are presented in Section 2. The ANFIS, ANN, and regression models are presented in Sections 3 and 4. The results and discussions are detailed in Section 5. Finally, the conclusions are presented in Section 6.

Experiments

A vertical CNC milling machine, a specially designed fixture, forming tools, and a piezoelectric dynamometer were used to conduct the experiments. The sheet material selected for this study was a commercial aluminum alloy, AA1050-H14, which is a popular grade of aluminum for general sheet metal work owing to its excellent corrosion resistance, high ductility, and highly reflective finish. Further, the material composition, extracted using a SPECTRO machine, is presented in Table 1. Tensile tests were conducted on the specimens using a Zwick/Roell universal testing machine, the results of which are presented in Table 2. The sheet was clamped using the designed fixture in a working area of 200 mm × 200 mm. The tool used during this process was cylindrical with a hemispherical head. In this study, the tool motion was controlled numerically. Therefore, the required part was designed using SOLIDWORK software, and the design was then transferred to MASTERCAM software to generate the toolpath. The numerical control (NC) codes were obtained from the generated toolpath and transferred to the CNC machine. For the accurate formation of parts, it is important to select the best toolpath, which in this case is a spiral toolpath. A truncated conical geometry was built with a base diameter of 100 mm and a height of 50 mm. Important parameters considered for the incremental sheet metal forming are tool diameter, sheet thickness, feed rate, and step size, the values of which are listed in Table 3.

Measuring the forming force during this process is extremely important to prevent failure, determine the optimal process, and implement on-line control. Forming force tests were conducted using a KISTLER 2825A1 with eight freely selectable measuring signal-component force dynamometer controllers, which helped measure the force components in three directions (x, y, and z). In addition, the measuring system included charge amplifiers (a complementary KISTLER 5019B three-channel charge amplifier) and data acquisition cards to record

Table 2. Measured mechanical properties of aluminum alloy AA1050-H14.

Material code	Yield Strength σy (MPa)	Ultimate Tensile Strength σUTS (MPa)	Elongation at Break A (mm)	Young Modulus E (MPa)
AA1050-H14	128	117.5	8.45	67648

https://doi.org/10.1371/journal.pone.0221341.t002

Table 3. Process parameters and their levels.

Input process parameters	Level 1	Level 2
Tool diameter (d)	10 mm	20 mm
Feed rate (f)	500 mm/min	1000 mm/min
Step size (s)	0.5 mm	1 mm
Sheet thickness (t)	1 mm	2 mm

https://doi.org/10.1371/journal.pone.0221341.t003

the measured forces on a PC. The sampling rate of the force measurement was 50 Hz. Fig 1 shows the experimental system and procedure used to measure the performance of the forming forces. The workpiece fixture was mounted on top of a piezoelectric load cell. The experimental results for all responses that were used as training and testing data for both the ANN and ANFIS models are listed in Table 4.

Development of predictive models for forming force

Adaptive neuro-fuzzy inference system

ANFIS is an effective approach to building models of complex nonlinear systems. Here, a hybrid learning process is used to structure an input–output mapping based on human knowledge and training data pairs. The ANFIS is applied in the framework of adaptive networks. It consists of five network layers. Each layer is described by several node functions. The information is moved unidirectionally. A diagram of the ANFIS structure with three inputs and two membership functions for each input and one output is shown in Fig 2. The objective of the current work is to investigate the potential of ANFIS in SPIF.

ANFIS consist of five layers to achieve the following fuzzy inference [32]:

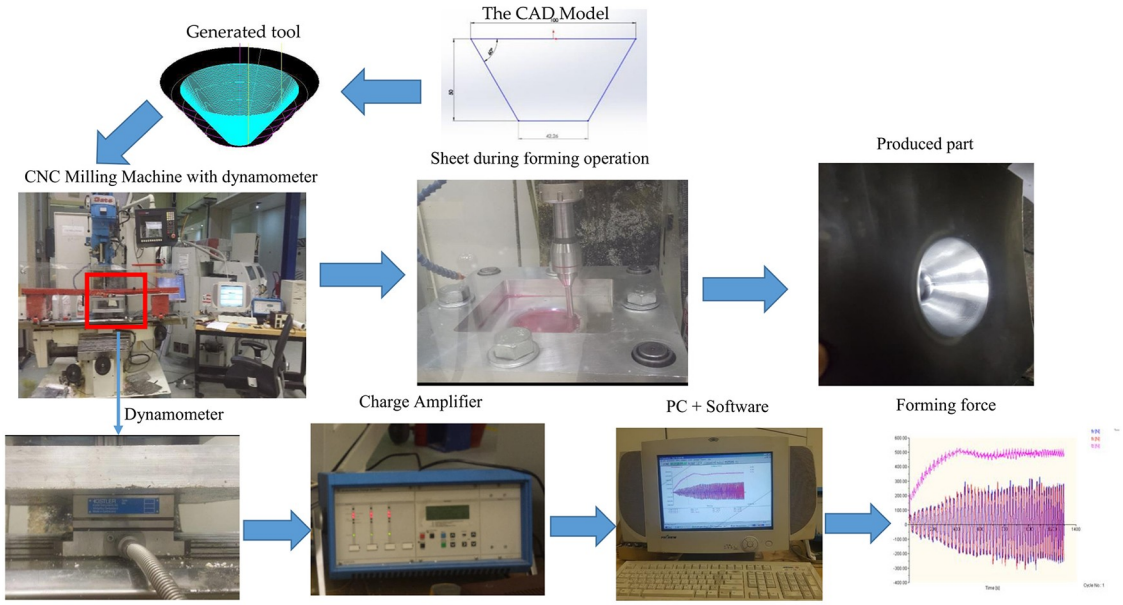

Fig 1. Experimental setup and forming force measurement.

https://doi.org/10.1371/journal.pone.0221341.g001

Table 4. Process parameters used with the corresponding experimental results of forming forces and predicted results.

Input Parameters				Experiment forming force			Predicted by ANFIS			Predicted by Regression			Predicted by ANN		
D	f	S	t	Fx (N)	Fy (N)	Fz (N)	Fx (N)	Fy (N)	Fz (N)	Fx (N)	Fy (N)	Fz (N)	Fx (N)	Fy (N)	Fz (N)
10	500	1	1	318.16	331.69	529.75	313	288	528	305.1563	313.846	393.83	133.6167	682.762	535.5682
20	1000	0.5	2	680.92	705.17	1636.29	681	692	1600	679.9625	718.428	1701.837	325.2577	305.312	1617.228
20	1000	0.5	1	313.98	304.99	525.67	318	305	562	316.9325	347.377	558.8969	177.1499	777.368	570.9501
20	500	0.5	2	779.79	770.42	1637.1	668	779	1600	751.625	709.889	1554.133	177.4208	200.635	1644.425
10	500	0.5	1	200.51	202.94	427.65	199	203	451	180.7838	196.024	484.765	194.3887	286.471	532.8672
10	500	0.5	1	197.09	214.55	474.92	199	203	451	180.7838	196.024	484.765	194.3887	239.491	532.8672
10	500	1	1	307.23	288.38	449.73	313	288	528	305.1563	313.846	393.83	133.6167	777.368	1644.425
20	500	0.5	1	323.41	323.65	520.47	372	249	296	388.595	261.341	411.1931	182.1449	168.643	417.5815
20	500	0.5	2	756.54	788.15	1651.34	668	779	1640	751.625	709.889	1554.133	177.1499	682.762	1617.228
10	1000	0.5	1	187.17	186.83	375.34	187	187	375	163.1713	157.298	359.975	202.9756	124.666	1644.413
20	1000	0.5	2	677.69	678.64	1587.21	681	692	1610	679.9625	718.428	1701.837	180.4025	124.666	319.592
10	1000	0.5	1	186.81	188.07	411.57	187	187	375	163.1713	157.298	359.975	134.2937	239.491	566.8363
20	500	1	2	420.7	447.42	873.51	338	365	770	449.615	466.56	934.7656	198.0989	373.817	584.791
20	500	0.5	1	420.7	173.59	295.76	372	249	296	388.595	261.341	411.1931	177.4208	152.6	509.3007
10	500	1	2	377.02	380.88	724.6	352	381	674	359.5638	295.91	685.505	246.7695	241.052	1618.019
20	1000	1	1	140.51	143.01	219.14	148	146	226	201.9425	106.683	304.7819	182.1449	605.412	363.1248
10	500	0.5	2	222.86	262.58	472.52	223	246	558	235.1913	315.321	565.99	180.4025	203.033	412.5591
10	1000	0.5	2	195.17	236.15	469.88	194	215	492	217.5788	199.098	441.2	173.8994	152.6	1618.019
20	1000	1	2	862.29	868.92	1631.76	619	612	1250	564.9725	594.368	1082.469	139.1313	149.039	570.9501
10	1000	1	2	258.35	270.47	564.92	258	292	572	208.5413	298.957	560.715	198.0989	147.722	363.1248
20	1000	1	2	375.95	355.04	863.46	619	612	1250	564.9725	594.368	1082.469	202.9756	277.943	566.8363
20	1000	0.5	1	321.2	329.46	598.28	318	305	532	316.9325	347.377	558.8969	130.9983	147.722	416.6108
10	500	1	2	327.03	331.91	622.96	352	381	674	359.5638	295.91	685.505	139.1313	152.6	251.8233
10	1000	1	2	257.48	292.22	579.96	258	292	572	208.5413	298.957	560.715	173.7338	124.666	584.791
20	500	1	1	157.15	160.28	239.35	157	159	237	86.585	155.244	157.0781	130.9983	241.052	1644.413
20	1000	1	1	155.08	148.48	234.16	148	146	226	201.9425	106.683	304.7819	189.5676	149.039	509.3007
20	500	1	2	338.47	364.73	665.74	338	365	770	449.615	466.56	934.7656	246.7695	361.18	412.5591
10	1000	0.5	2	192.35	215.09	513.93	194	215	492	217.5788	199.098	441.2	130.5799	305.312	615.1648
10	1000	1	1	112.52	111.6	176.58	113	101	174	154.1338	140.523	269.04	134.2937	373.817	251.8233
20	500	1	1	156.08	157.83	231.07	157	159	237	86.585	155.244	157.0781	130.5799	200.635	412.5591
10	1000	1	1	97	91.32	169.68	113	101	174	154.1338	140.523	269.04	173.7338	203.033	417.5815
10	500	0.5	2	211.49	229.27	558.05	223	246	558	235.1913	315.321	565.99	189.5676	277.943	319.592

https://doi.org/10.1371/journal.pone.0221341.t004

Layer 1: Fuzzy layer

In this layer, the membership value is calculated using the following equation:

$$\mu Ai(x) = \frac{1}{1 + [\left(\frac{x - c_i}{a_i}\right)^2]^{b_i}}, \tag{1}$$

where $\mu\ A_i(x)$ is an appropriate parameterized membership function, and a_i, b_i, and c_i form a parameter set that changes the forms of the functional movement screen () with a value between 1 and 0.

Layer 2: Multiplies the incoming signals and sends the product out.

$$i = \mu Ai(x) \ \times \mu\ B_i(y) \times \ \mu\ C_i(z), \ \ i = 1, 2, \tag{2}$$

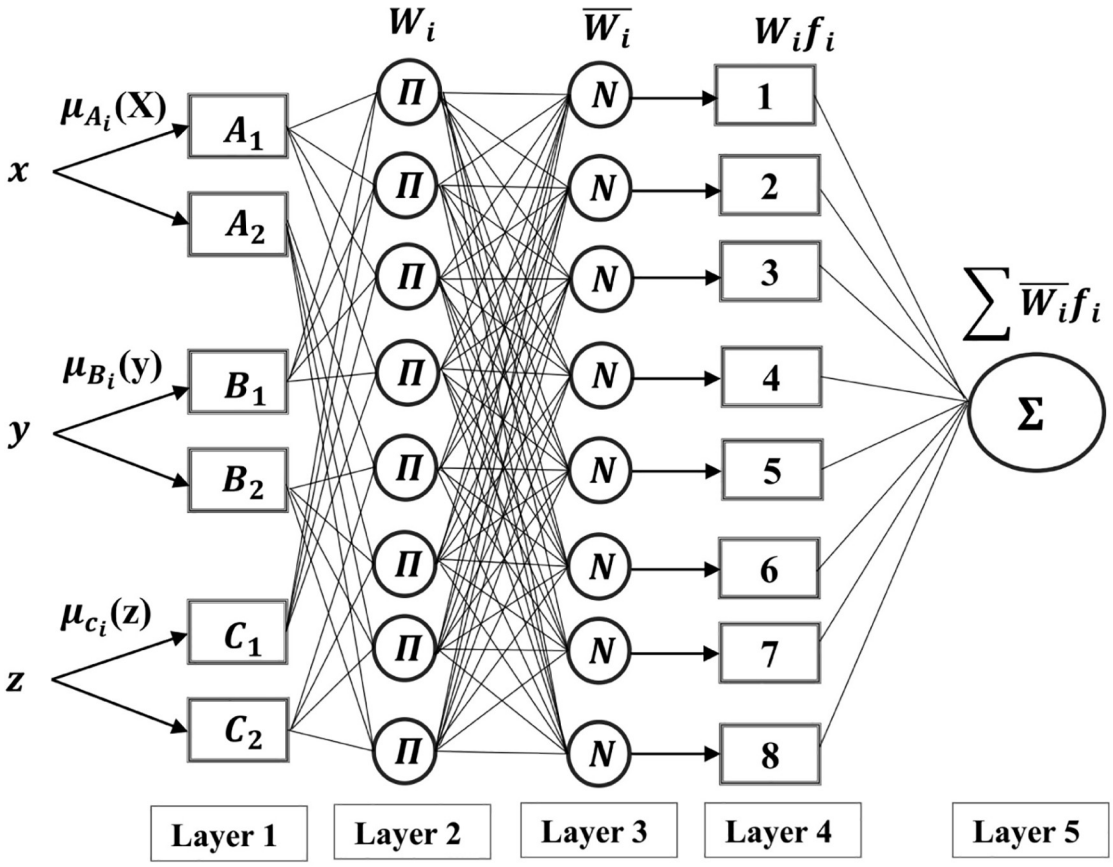

Fig 2. ANFIS architecture with five layers and several nodes [32].

https://doi.org/10.1371/journal.pone.0221341.g002

Each node output represents the firing strength of a rule.

Layer 3: Normalizes the firing strengths

In this layer, the normalized firing strength is computed using the following equation:

$$\bar{w}_i = \frac{w_i}{\sum_i w_i} \quad , \quad i = 1, 2, \tag{3}$$

where w_i denotes the output of layer i.

Layer 4: Defuzzification

In this layer, each node i is an adaptive node with a node function.

$$\bar{w}_i.f_i = \bar{w}_i.(p_i.x + q_i.y + r_i.z + s_i), \tag{4}$$

where p_i, q_i, r_i, and s_i make up the consequent parameter set of the node, which are identified during the training process.

Layer 5: Total output layer

In this layer, all incoming signals are added (summation output). The circle node function

is fixed whereas the indicated square function is adaptive. This can be calculated as follows:

$$\text{Overall output} = \sum_i \bar{w}_i f_i = \frac{\sum_i w_i f_i}{\sum_i w_i}, \quad i = 1, 2, \tag{5}$$

Neural network model used for prediction

The ANN computational model involves three layers, output, hidden, and input layers. Each layer contains neurons and each neuron is related to all the neurons in the next layer. Fig 3 shows the layers in a model of the forming force (Fz).

None of the processes are executed in the input layer, and the input for the neuron is obtained from the actual setting. The input vector is the weight of a neuron multiplied by the strength; the result obtained helps create the product. The output from the last neuron can be interconnected to the input of the next neurons or can be directly interconnected with the environment. The output comprises an activation function and a summation function. The activation function takes the weight of a neuron as an input and produces its activation as an output. The calculation of the net input from the processing neurons is the summation function. Using the ANN, the nonlinear relationships between the output and input owing to the contained activation function of the nonlinear and linear algebraic equations can be stored. After the weight is altered by the activation function, the neurons that have moved to other neurons make up the next layer. The output of the activation function accepts the results, and then presents them to either the external network or to the neurons in the next layer. The network output is compared with the target having the applied input, and the difference between them is then considered an error. Moreover, algorithms of different networks are applied to decrease the error [33].

Result and discussions

Statistical analysis

An analysis of variance (ANOVA) was used to estimate the effects of all factors and their interaction on Fz. As a standard practice in ANOVA, terms with a p-value $< \alpha = 0.05$ are

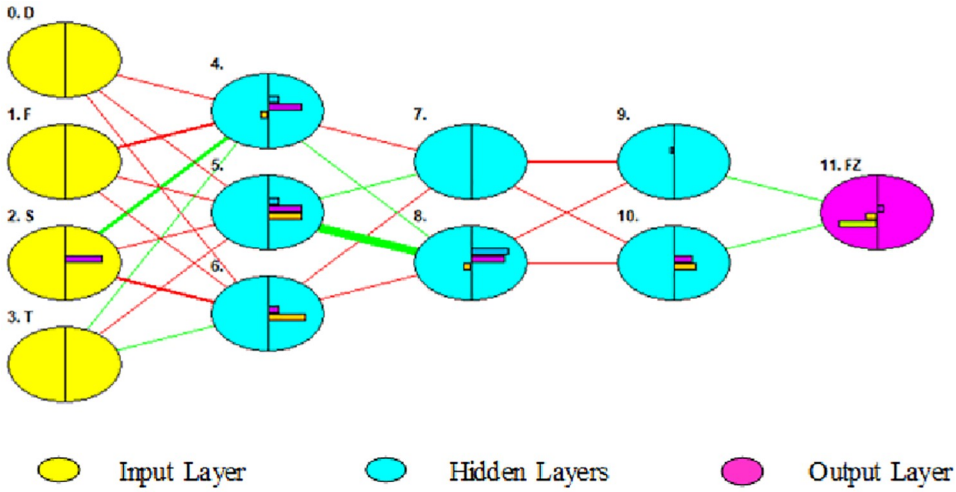

Fig 3. Neural network model for Fz.

https://doi.org/10.1371/journal.pone.0221341.g003

Table 5. ANOVA results for Fz.

Source	DF	Adj SS	Adj MS	F-Value	P-Value
Model	9	6002399	666933	25.34	0
Linear	4	4071606	1017901	38.67	0
d	1	1083491	1083491	41.16	0
f	1	1050	1050	0.04	0.844
s	1	356930	356930	13.56	0.001
t	1	2630134	2630134	99.92	0
2-Way Interactions	4	1765076	441269	16.76	0
d*f	1	148506	148506	5.64	0.027
d*s	1	406858	406858	15.46	0.001
d*t	1	1197730	1197730	45.5	0
s*t	1	11982	11982	0.46	0.507
3-Way Interactions	1	165717	165717	6.3	0.02
d*s*t	1	165717	165717	6.3	0.02
Error	22	579085	26322		
Lack-of-Fit	6	218117	36353	1.61	0.208
Pure Error	16	360968	22561		
Total	31	6581484			
Model Summary	S 162.241 R-sq 91.20% R-sq(adj) 87.60%				

https://doi.org/10.1371/journal.pone.0221341.t005

considered significant. The ANOVA results, presented in Table 5, indicate that the factors d, s, and t; the two-way interactions d*f, d*s, and d*t; and the three-way interaction between d, s, and t have a significant effect on Fz. The value of the adjusted R-squared value shows that the model can explain 91% of the variations in the data, and that 9% of the variations originate from unknown nuisance factors.

ANFIS results

The ANFIS model was developed as a function of SPIF for the forming force using training and testing data. The ANFIS tool that already exists in MATLAB was applied, which tests the relationship of the process parameters used to execute the perfect training and maximizes the prediction model accuracy for the selected responses (forming force). To obtain the results, the ANFIS algorithm was designed using the initial parameters. Table 6 lists the parameters used to help build the ANFIS model.

The training process was applied using 100 epochs for the forming force on three axes (Fx, Fy, and Fz). A training curve was obtained after the training process was complete, as shown in Fig 4. The figure shows the relationship between the number of epochs and the errors in the responses.

Table 6. Initial parameters for the construction of the ANFIS.

Responses	Forming force		
	Fx	Fy	Fz
Training method	hybrid	hybrid	hybrid
Membership function for inputs	gaussmf	trimf	psigmf
Number of membership function	3 2 3 1	2 2 2 2	3 3 3 3
Output function	constant	constant	constant
Number of epochs	100	100	100

https://doi.org/10.1371/journal.pone.0221341.t006

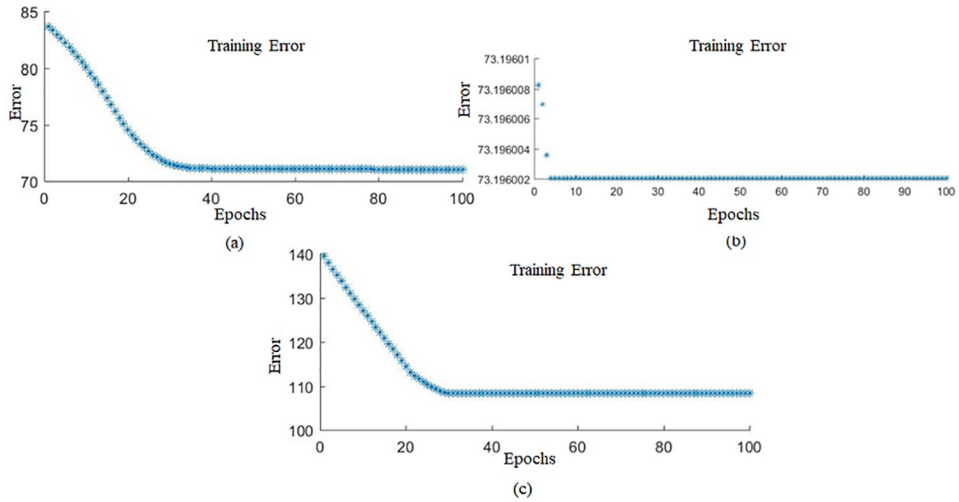

Fig 4. ANFIS training curve for forming force: (a) Fx, (b) Fy, and (c) Fz.

https://doi.org/10.1371/journal.pone.0221341.g004

An analysis of the curves shows that, after 35 epochs, the errors become steady, as shown in Fig 4(a). This occurs because the developed model was trained using limited experimental data. To obtain the initial predicted values of the outputs, such as the forming force, a set of fuzzy inference parameters (FIPs) were selected during the training process. The measured values were compared with the predicted value of the forming force obtained from the developed ANFIS model. The performance of this model was measured based on the difference between the measured and predicted values.

During the training process, FIPs were repeated multiple times until the errors were minimized. Different ANFIS parameters were used as the training parameters to validate the accuracy of the prediction model. Table 7 shows the different ANFIS architectures for a predictive

Table 7. Different ANFIS architectures for forming force.

Responses	NO. MF	Type of MF	Output function	Errors RMSE	
				Training error	Test error
Forming force (Fx)	3 3 3 3	trimf	constant	73.196	31.4218
			linear	73.196	31.4166
	2 2 2 2	Trapmf	constant	73.4195	33.2606
	3 3 3 3		constant	73.196	31.4218
	3 3 3 3	psigmf	constant	73.196	31.4309
Forming force (Fy)	2 2 2 2	trimf	constant	108.9255	103.2906
	2 2 2 2		linear	108.3141	104.6017
	3 3 3 3	trapmf	constant	108.3141	104.5998
	2 2 2 2		constant	108.3236	104.2812
	2 2 2 2	psigmf	constant	108.3145	104.5399
	3 3 3 3		constant	108.3141	104.5998
Forming force (Fz)	3 3 3 3	psigmf	Constant	70.7654	32.4088
	3 3 2 1		linear	96.5383	105.72
	2 2 2 2	gaussmf	constant	70.2728	31.9748
	3 3 3 3		constant	71.018	37.5940
	3 3 3 3	trapmf	constant	71.0169	31.8061
	3 2 3 1	gaussmf	constant	172.7283	131.9702

https://doi.org/10.1371/journal.pone.0221341.t007

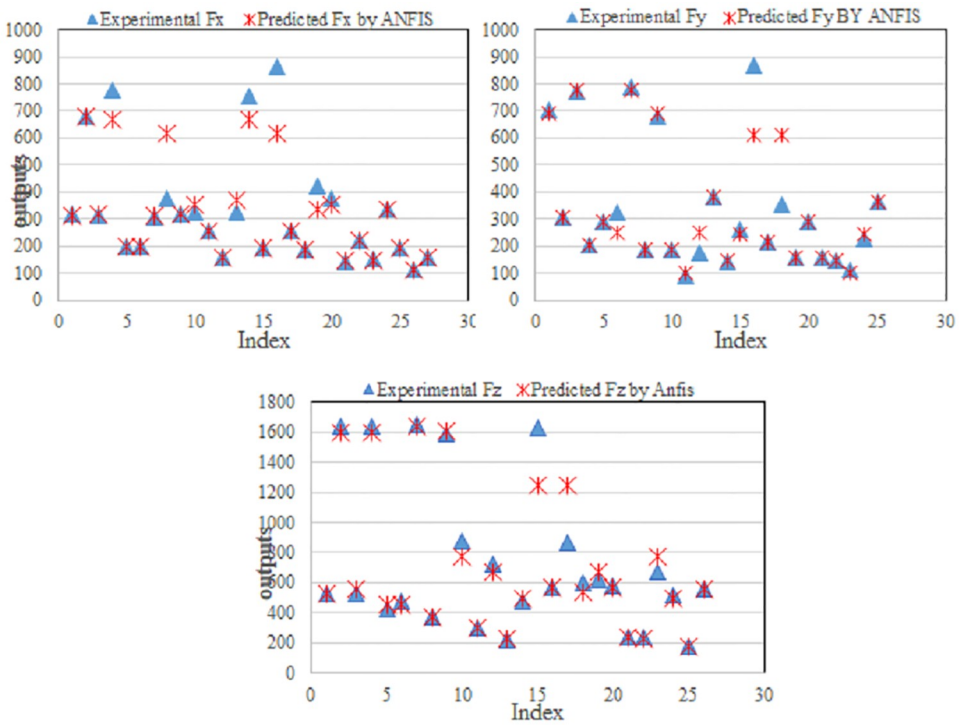

Fig 5. Comparison between the measured and predicted forming forces using the ANFIS training data.

https://doi.org/10.1371/journal.pone.0221341.g005

model of the forming forces obtained for different input membership shapes, numbers of membership functions, and types of output (linear or constant). For instance, from Table 7, the trimf function was chosen to train the ANFIS because it achieved the lowest testing error of 31.4218. In addition, Figs 5 and 6 show a comparison between the measured and predicted forming forces for the training and testing data.

Artificial neural network results

The results of the developed ANN model are used to predict the forming force based on the input process parameters in single-point incremental sheet metal forming. The numbers of training and testing samples are 28 and 6, respectively.

Several training experiments were carried out to identify the optimal network structure and best training parameters of the neural networks, producing minimum errors during the training phase. Similarly, several training experiments with different numbers of hidden neurons, learning rates (0.60), and momentum values (0.80) were checked, as shown in Fig 7. The graph of the learning progress shows the maximum, average, and minimum training errors. The average validation error is 0.00138, which was obtained for a maximum of 38,650,000 learning cycles. The correlation coefficient (R value) can be used to gauge the performance of the established network. The R value is between the measured value and the predicted value for the testing (6) and training data (28). The measurement of the closeness of the dissimilarity in the output clarified by the target is known as the R value, which lies between 1 and 0. When the R value equals 1, the optimal correlation is observed between the output and target values for the forming force on the three axes. The R value obtained between the predicted values and the measured data is 0.981, which indicates a good correlation.

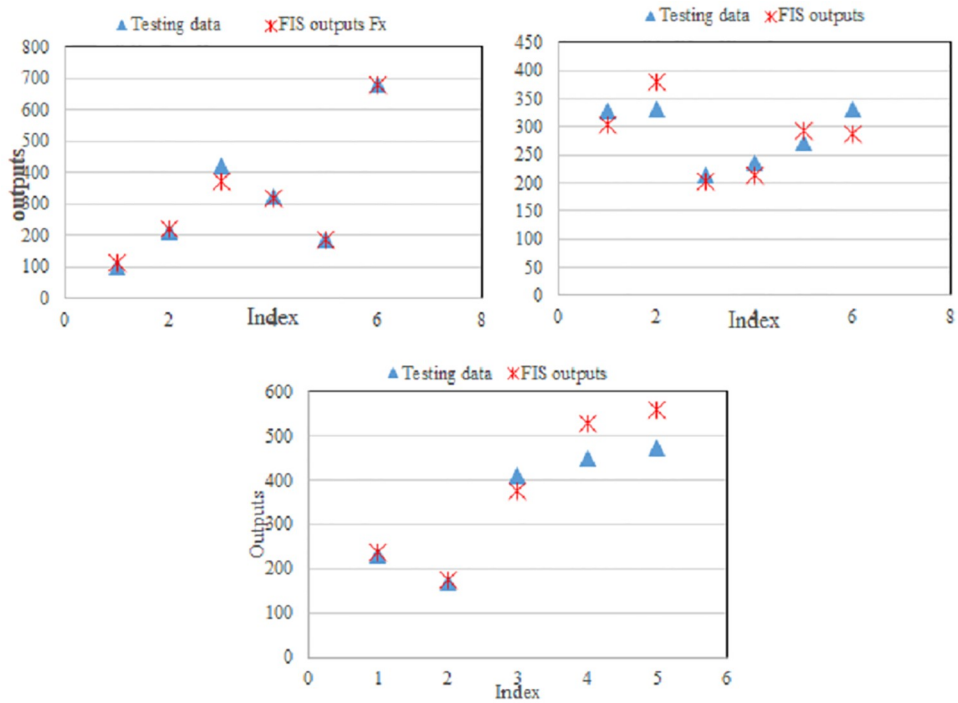

Fig 6. Comparison between the measured and predicted forming force using the ANFIS test data.

https://doi.org/10.1371/journal.pone.0221341.g006

Regression model

A regression analysis helps in the development of a mathematical equation to characterize the relationship between two or more input variables and the response outputs. In this study, mathematical models are also developed using a regression analysis to fit the measured data for the three selected responses. Using Minitab software, regressions models for the forming force were developed, and a full quadratic model was initially selected for all responses. Later, the insignificant terms were removed based on their p-values and accuracy. The following equations can be used to predict the forming force as a function of significant factors:

$$\begin{aligned} F_x(N) = &-814 + 70.0d + 0.981f + 2009\ s - 254.2\ t - 0.0749d * f \\ &- 149.4\ d * s + 30.86\ d * t - 1.815\ f * s + 0.1282\ d * f * s, \end{aligned} \tag{6}$$

$$\begin{aligned} F_y(N) = &-441 + 16.5d + 0.605\ f + 1735\ s + 259\ t + 0.0250\ d * f - 44.8\ d * s \\ &+ 32.93\ d * t - 32.93\ f * s - 0.663\ f * t - 782\ s * t + 1.015\ f * s * t, \end{aligned} \tag{7}$$

$$\begin{aligned} F_z(N) = &\ 2650 + 182.0\ d - 0.795\ f + -1428\ s - 1767\ t + \ 0.0545\ d * f \\ &+ 82.5\ d * s + 163.7\ d * t + \ 1572\ s * t - 115.1\ d * s * t, \end{aligned} \tag{8}$$

Comparison of ANFIS with ANN and regressions

To assess the ability of the developed ANFIS model relative to that of a neural network and regression analysis, an ANN model and a regression algorithm were developed using the same input variables. Table 4 summarizes the results. For the forming force model along the x-axis, Fig 8 shows a comparison between the measured and predicted values obtained using the

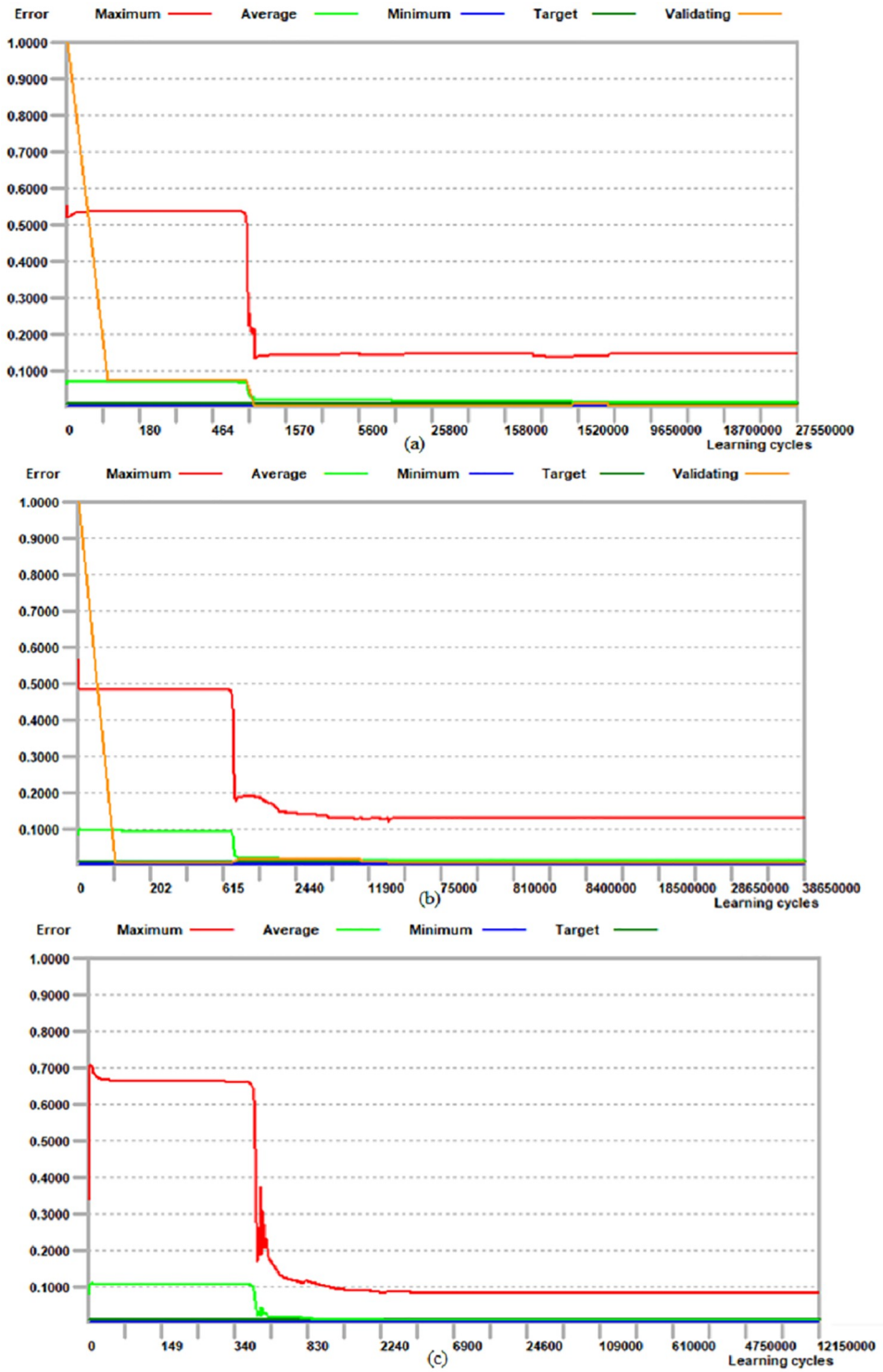

Fig 7. ANN training curve for forming force.

https://doi.org/10.1371/journal.pone.0221341.g007

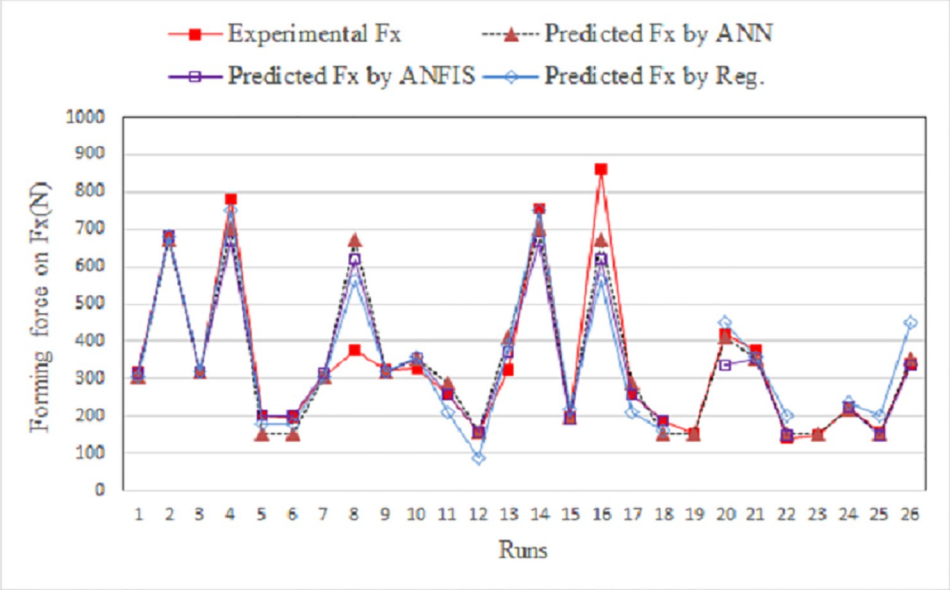

Fig 8. Comparison between experimental and predicted Fx for training data.

https://doi.org/10.1371/journal.pone.0221341.g008

ANFIS, ANN, and regressions models for the training data. Fig 9 shows the same for the testing data.

Fig 10 shows a comparison between the measured and predicted values obtained using ANFIS and the regression model for the training data. Fig 11 shows the same for the testing data.

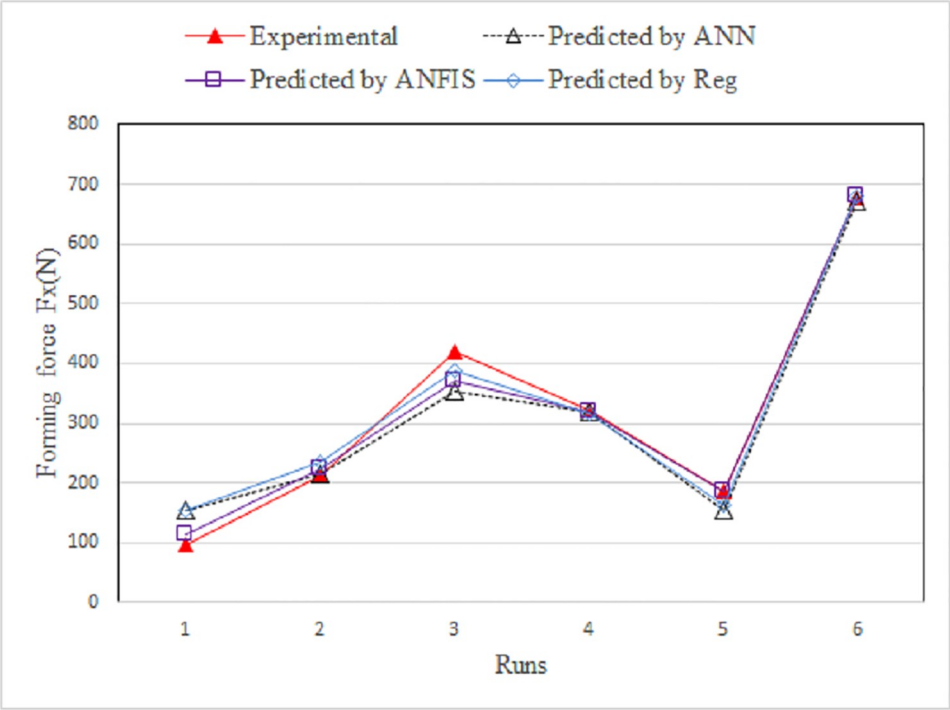

Fig 9. Comparison between measured and predicted Fx for testing data.

https://doi.org/10.1371/journal.pone.0221341.g009

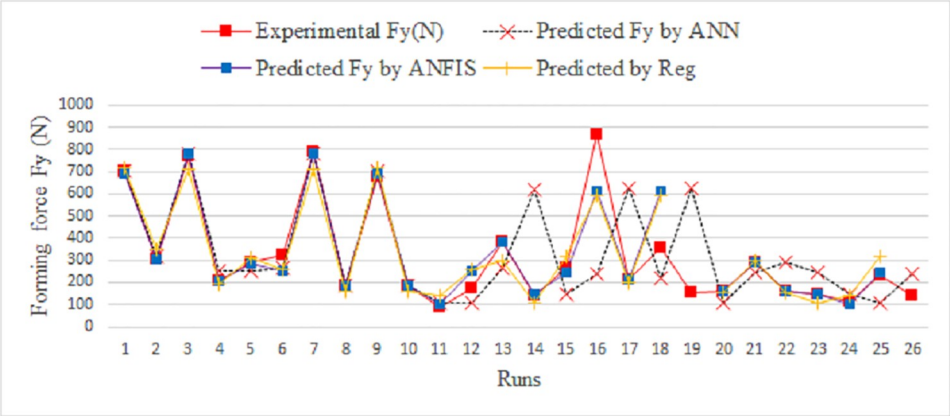

Fig 10. Comparison between measured and predicted Fy for training data.

https://doi.org/10.1371/journal.pone.0221341.g010

Fig 12 shows a comparison between the measured and predicted values obtained using ANFIS and the regression model for the training data. Fig 13 shows the same for the testing data.

The results obtained using the ANFIS prediction are very close to the measured values. Moreover, the absolute mean percentage errors were calculated for each of the developed models. Tables 8 and 9 present a comparison of the performance between the ANFIS, ANN, and regression models based on the mean absolute percentage errors (MAPE) for the training and testing data.

Based on the performances of the ANFIS and ANN models in terms of the average absolute percentage error for the training and testing data, it was observed that the ANFIS model outperforms the ANN and regression models, while retaining their full potential.

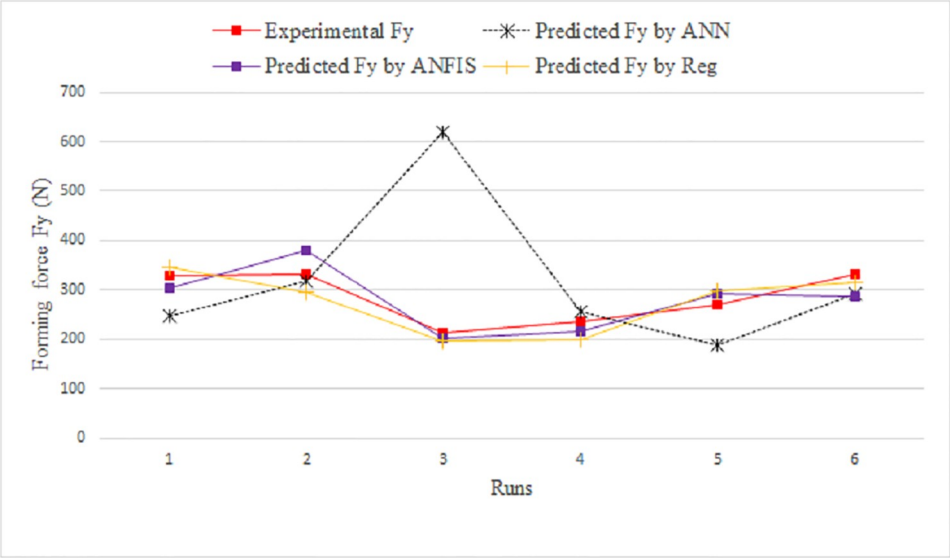

Fig 11. Comparison between measured and predicted Fy for testing data.

https://doi.org/10.1371/journal.pone.0221341.g011

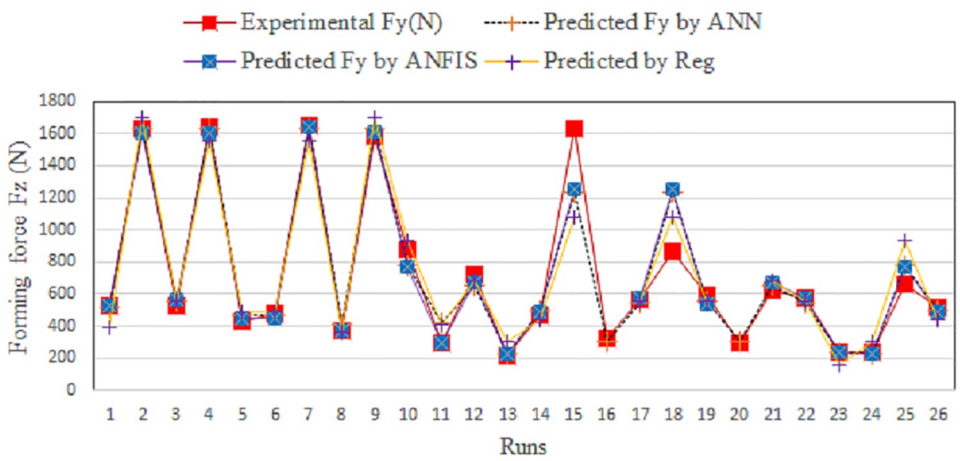

Fig 12. Comparison between measured and predicted Fz for training data.

https://doi.org/10.1371/journal.pone.0221341.g012

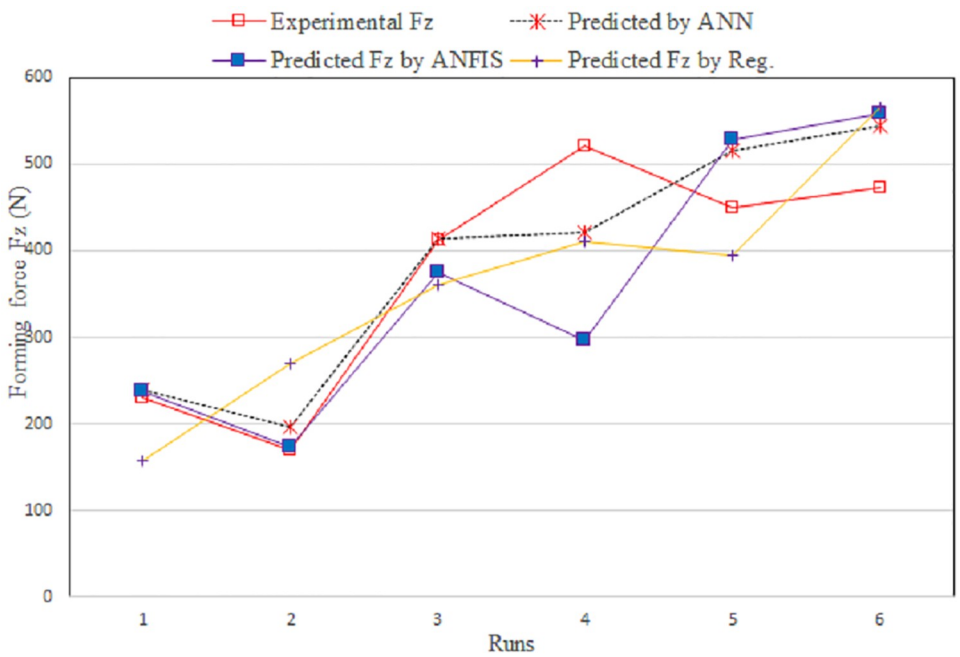

Fig 13. Comparison between experimental and predicted Fz for testing data.

https://doi.org/10.1371/journal.pone.0221341.g013

Table 8. Comparison of the developed models based on the mean absolute percentage errors for training data.

Outputs	ANFIS model	ANN model	Reg. model
	MAPE	MAPE	MAPE
Forming force Fx	7.25	12.04	18.08
Forming force Fy	8.25	55.73	19.55
Forming force Fz	6.42	8.98	16.27

https://doi.org/10.1371/journal.pone.0221341.t008

Table 9. Comparison of the developed models based on the mean absolute percentage errors for testing data.

Outputs	ANFIS model	ANN model	Reg. model
	MAPE	MAPE	MAPE
Forming force Fx	5.85	16.14	15.37
Forming force Fy	9.61	44.77	9.42
Forming force Fz	15.44	11.59	26.05

https://doi.org/10.1371/journal.pone.0221341.t009

Conclusions

This paper proposed ANFIS and ANN models to predict the forming force in the context of sheet metal forming, particularly SPIF. In addition, the influences of the tool diameter, feed rate, sheet thickness, and step size on the main forming force were investigated. Considering the ANOVA for the forming force (Fz), it was concluded that the significant factors are the tool diameter, step size, and sheet thickness. The results of the ANFIS and ANN models were compared with both the experimental data and those predicted using a regression model. The comparison showed that the ANFIS model can accurately predict the forming force for both training and testing data; in addition, the ANFIS model exhibited a better prediction performance for the selected responses. Moreover, the results showed that the ANFIS model can predict the forming force along the three axes for the training data with a MAPE of 7.25%, 6.42%, and 8.98%, respectively, and for the testing data with a MAPE of 5.85%, 9.61%, and 15.44%, respectively. It can therefore be concluded that the developed model using the ANFIS approach can be effectively used to measure the forming force during ISF and provide more reliable results than the ANN and regression models.

Acknowledgments

The authors extend their appreciation to the Deanship of Scientific Research at King Saud University for funding this work through research group no. (RG-1439-56).

The authors also thank the Deanship of Scientific Research and RSSU at King Saud University for their technical support.

Author Contributions

Conceptualization: Ali Alsamhan, Adham E. Ragab, Abdulmajeed Dabwan, Mustafa M. Nasr, Lotfi Hidri.

Data curation: Ali Alsamhan, Adham E. Ragab, Abdulmajeed Dabwan, Mustafa M. Nasr.

Investigation: Ali Alsamhan, Adham E. Ragab, Abdulmajeed Dabwan, Mustafa M. Nasr.

Methodology: Ali Alsamhan, Adham E. Ragab, Abdulmajeed Dabwan, Mustafa M. Nasr.

Supervision: Ali Alsamhan, Adham E. Ragab, Lotfi Hidri.

Validation: Adham E. Ragab.

Visualization: Abdulmajeed Dabwan, Mustafa M. Nasr.

Writing – original draft: Abdulmajeed Dabwan, Mustafa M. Nasr.

Writing – review & editing: Ali Alsamhan, Adham E. Ragab, Lotfi Hidri.

References

1. Tomaž P. Numerical analyses of tube hydroforming by high internal pressure. Strojniški vestnik—Journal of Mechanical Engineering. 2004; 50(1):31–43.
2. Tomaž P, Zlatko K. Analysing the quality of sheet-metal holding during deep drawing. Strojniški vestnik —Journal of Mechanical Engineering. 2001;94–105.
3. Jeswiet J, Micari F, Hirt G, Bramley A, Duflou J, Allwood J. Asymmetric single point incremental forming of sheet metal. CIRP Ann. 2005; 54(2):88–114.
4. Bambach, Hirt G, Junk S. Modelling and experimental evaluation of the incremental cnc sheet metal forming process. Conference on Computational Plasticity (COMPLAS). 2003.
5. Amino H, Lu Y, Ozawa S, Fukuda K, Maki T. Dieless NC forming of automotive service panels. International conference; 7th, Technology of plasticity. 2002;1015–1020
6. Lievers WB, Pilkey AK, Lloyd DJ. Using incremental forming to calibrate a void nucleation model for automotive aluminum sheet alloys. Acta Materialia 2004; 52(10):3001–3007.
7. Tanaka S, Nakamura T, Hayakawa K, Nakamura H, Motomura K. Residual stress in sheet metal parts made by incremental forming process. AIP Conference Proceedings 2007;775–80.
8. Ambrogio G, De Napoli L, Filice L, Gagliardi F, Muzzupappa M. Application of incremental forming process for high customised medical product manufacturing. Journal of Materials Processing Technology. 2005; 162–163:156–162.
9. Oleksik V, Pascu A, Deac C, Fleaca R, Roman M, Bologa O, et al. The influence of geometrical parameters on the incremental forming process for knee implants analyzed by numerical simulation. AIP Conference Proceedings. 2010;1208–15.
10. Petek A, Kuzman K, Kopaè J. Deformations and forces analysis of single point incremental sheet metal forming. Archives of Materials Science and Engineering. 2009; 35(2);107–116.
11. Li Y Le, Liu ZB, Lu HB, Daniel WJTB, Meehan PA. Experimental study and efficient prediction on forming forces in incremental sheet forming. Advanced Materials Research. 2014; 939:313–21.
12. Iseki H. An approximate deformation analysis and FEM analysis for the incremental bulging of sheet metal using a spherical roller. J Mater Process Technol. 2001; 111(1–3):150–4.
13. Jeswiet J, Duflou J, Szekeres A. Forces in single point and two point incremental forming [Internet]. 2005.
14. Filice L, Ambrogio G, Micari F. On-line control of single point incremental forming operations through punch force monitoring. CIRP Ann 2006; 55(1):245–8.
15. Dabwan A. Determining the effect of key process parameters on forming force of single point incremental sheet metal forming. International Conference on Industrial Engineering and Operations Management. 2016;2833–2840.
16. Duflou J, Tunçkol Y, Szekeres A, Vanherck P. Experimental study on force measurements for single point incremental forming. J Mater Process Technol. 2007; 189(1–3):65–72.
17. Kumar A, Gulati V. Experimental investigations and optimization of forming force in incremental sheet forming. Sadhana—Academy Proceeding in Engineering Science. 2018; 43(10).
18. Bagudanch I, Centeno G, Vallellano C, Garcia-Romeu ML. Forming force in single point incremental forming under different bending conditions. Procedia Eng. 2013 J; 63:354–60.
19. Arfa H, Bahloul R, BelHadjSalah H. Finite element modelling and experimental investigation of single point incremental forming process of aluminum sheets: Influence of process parameters on punch force monitoring and on mechanical and geometrical quality of parts. Int J Mater Form. 2013; 6(4):483–510.
20. Henrard C, Bouffioux C, Eyckens P, Sol H, Duflou JR, Van Houtte P, et al. Forming forces in single point incremental forming: Prediction by finite element simulations, validation and sensitivity. Comput Mech. 2011; 47(5):573–90.
21. Ingarao G, Ambrogio G, Gagliardi F, Di Lorenzo R. A sustainability point of view on sheet metal forming operations: Material wasting and energy consumption in incremental forming and stamping processes. J Clean Prod. 2012; 29–30:255–68.
22. Petek A, Kuzman K, Suhač B. Autonomous on-line system for fracture identification at incremental sheet forming. CIRP Ann. 2009; 58(1):283–6.
23. Fiorentino A. Force-based failure criterion in incremental sheet forming. Int J Adv Manuf Technol. 2013; 68(1–4):557–63.
24. Ambrogio G, Filice L, Micari F. A force measuring based strategy for failure prevention in incremental forming. J Mater Process Technol. 2006; 177(1–3):413–6.
25. Kar S, Das S, Kanti P. Applications of neuro fuzzy systems: A brief review and future outline. Appl Soft Comput J. 2014; 15:243–59.

26. Jang J-SR. Fuzzy Modeling using generalized neural networks and kalman filter algorithm. AAAI-91 Proceedings. 1991;762–7.

27. Abraham A. Adaptation of fuzzy inference system using neural learning. Fuzzy Systems Engineering. 2005; 181:53–83.

28. Anwar S, Nasr MM, Alkahtani M, Altamimi A. Predicting surface roughness and exit chipping size in BK7 glass during rotary ultrasonic machining by adaptive neuro-fuzzy inference system (ANFIS). In: Proceedings of the International Conference on Industrial Engineering and Operations Management. 2017.

29. Kurra S, Hifzur Rahman N, Regalla SP, Gupta AK. Modeling and optimization of surface roughness in single point incremental forming process. J Mater Res Technol. 2015; 4(3):304–13.

30. Do VC, Kim YS. Effect of hole lancing on the forming characteristic of single point incremental forming. Procedia Eng. 2017; 184:35–42.

31. Khan MS, Coenen F, Dixon C, El-Salhi S, Penalva M, Rivero A. An intelligent process model: Predicting springback in single point incremental forming. Int J Adv Manuf Technol. 2015; 76(9–12):2071–82.

32. Syukor A, Jaya M, Samad A, Basari H, Zaiton S, Hashim M, et al. Application of ANFIS in predicting of TiAlN coatings hardness department of industrial computing. Australian Journal of Basic and Applied Sciences. 2011; 5(9):1647–1657.

33. Kant G, Singh K. Predictive modelling and optimization of machining parameters to minimize surface roughness using artificial neural network coupled with genetic algorithm. Procedia CIRP. 2015; 31:453–8.